JPET Fast Forward. Published on January 23, 2012 as DOI: 10.1124/jpet.111.189340

JPET #189340

Hypoxia-inducible Factor Activation in Myeloid Cells Contributes to the Development of Liver Fibrosis in Cholestatic Mice

Bryan L. Copple, Sophia Kaska, and Callie Wentling

Department of Pharmacology, Toxicology, and Experimental Therapeutics, University of Kansas Medical Center, Kansas City, KS 66160

Running Title Page

a) Role for Myeloid HIFs in Liver Fibrosis

b) Corresponding Author/Author to receive reprint requests:

Bryan L. Copple

Department of Pharmacology & Toxicology

Michigan State University

B403 Life Sciences Building

East Lansing, MI 48823

Phone: (517)884-6691

Fax: (517)353-8915

E-mail: copple@msu.edu

c) Number of text pages: 31

Number of tables: 4

Number of figures: 9

Number of references: 37

Number of words in Abstract: 239

Number of words in Introduction: 498

Number of words in Discussion: 1109

d) Nonstandard abbreviations: hypoxia-inducible factor (HIF), platelet-derived growth factor-B (PDGF-B), transforming growth factor-β (TGF-β), bile duct ligation (BDL), primary biliary cirrhosis (PBC), primary sclerosing cholangitis (PSC), monocyte chemotactic protein-1 (MCP-1), alanine aminotransferase (ALT), smooth muscle actin (SMA), plasminogen activator inhibitor-1 (PAI-1), fibroblasts growth factor-2 (FGF-2),

JPET Fast Forward. Published on January 23, 2012 as DOI: 10.1124/jpet.111.189340
This article has not been copyedited and formatted. The final version may differ from this version.

keratinocyte-derived chemotactic factor (KC), macrophage inflammatory protein-2 (MIP-2), tumor necrosis factor-α (TNF-α), angiopoietin (Ang), vascular endothelial growth factor-A (VEGF-A)

e) Recommended section: Gastrointestinal, Hepatic, Pulmonary, and Renal

Abstract

Macrophages play an integral role in the development of liver fibrosis by releasing mediators, such as platelet-derived growth factor-B (PDGF-B) and transforming growth factor-β1, which stimulate hepatic stellate cell proliferation, chemotaxis, and collagen production. The mechanism by which chronic liver injury stimulates macrophages to release these mediators, however, is not completely understood. We tested the hypothesis that chronic liver injury activates hypoxia-inducible factor (HIF) transcription factors in macrophages that regulate production of mediators that promote fibrosis. To test this hypothesis, Cre/lox technology was used to generate myeloid cell-specific HIF-1α or HIF-1β knockout mice. When these mice were subjected to bile duct ligation (BDL), levels of α-smooth muscle actin and type I collagen in the liver were reduced when compared to mice with normal levels of HIFs. Deficiency of HIFs in macrophages did not affect liver injury or inflammation after BDL, but reduced platelet-derived growth factor-B (PDGF-B) mRNA and protein, suggesting that HIF activation in macrophages may promote fibrosis by regulating production of PDGF-B. Consistent with a role for HIFs in liver fibrosis in cholestatic liver disease, nuclear HIF-1α protein was present in macrophages, hepatocytes, and fibroblasts in livers from patients with primary biliary cirrhosis (PBC) and primary sclerosing cholangitis (PSC). These studies demonstrate that HIFs are important regulators of profibrotic mediator production by macrophages during the development of liver fibrosis, and suggest that HIFs may be a novel therapeutic target for the treatment of chronic liver disease in patients.

Introduction

Humans are exposed to a variety of chemicals, pathogens, or conditions that produce chronic liver injury, including alcohol, hepatitis viruses, autoimmune diseases, and genetic disorders. The liver responds to injury by producing soluble mediators, such as growth factors, that facilitate liver repair (Fausto, 2000). This process is essential for restoration of liver homeostasis following acute injury. During chronic injury, however, persistent activation of these pathways promotes pathological processes, including fibrosis and cancer (Friedman, 2008).

Macrophages play an integral role in the development of liver fibrosis. Studies have shown that depletion of macrophages slows the progression of fibrosis in animal models (Rivera et al., 2001; Duffield et al., 2005). The mechanism by which macrophages promote fibrosis is not completely understood, although, studies have shown that these cells express key mediators of fibrosis, such as platelet-derived growth factor-B (PDGF-B) and transforming growth factor-β (TGF-β) (Nakatsukasa et al., 1990; Faiz Kabir Uddin Ahmed et al., 2000). Accordingly, macrophages may promote fibrosis by releasing profibrotic growth factors that stimulate hepatic stellate cells and peribiliary fibroblasts to become activated and to produce collagen. What remains to be identified, however, is the mechanism by which chronic liver injury stimulates macrophages to produce mediators that promote fibrosis. Our recent studies suggest that hepatocellular hypoxia may be important for this process.

Several studies have demonstrated that hepatocellular damage causes regions of hypoxia to develop in liver (Ji et al., 1982; Rosmorduc et al., 1999; Corpechot et al., 2002; Copple et al., 2004; Moon et al., 2009; Rosmorduc and Housset, 2010). We recently demonstrated that exposure of Kupffer cells to hypoxia *in vitro* increased expression of PDGF-B, a potent mitogen and chemotaxin for hepatic stellate cells, and monocyte chemotactic protein-1 (MCP-1), a mediator of hepatic stellate cell chemotaxis (Copple et al., 2010). This

study suggested that hypoxia may be a key driving force for the production of profibrotic mediators by macrophages during fibrosis. These studies further demonstrated that upregulation of PDGF-B and MCP-1 in hypoxic Kupffer cells required the transcription factor hypoxia-inducible factor-1α (HIF-1α) (Copple et al., 2010).

HIFs are a group of transcription factors activated in hypoxic cells (Semenza and Wang, 1992; Gaber et al., 2005; Coleman and Ratcliffe, 2007). The functional HIF transcription factor is composed of an α subunit, either HIF-1α or HIF-2α, and a β subunit, HIF-1β. When cells become hypoxic, HIF-α protein subunits become stabilized and translocate to the nucleus where they heterodimerize with HIF-1β and regulate expression of genes that allow cells to adapt to a hypoxic environment (Cash et al., 2007). Our recent studies demonstrated that HIF-1α is activated in macrophages in the livers of bile duct-ligated (BDL) mice, an animal model of peribiliary fibrosis (Moon et al., 2009). Whether activation of HIF-1α in hepatic macrophages *in vivo* is a key event in the development of liver fibrosis, however, is not known. Accordingly, in the present study, the hypothesis was tested that HIF-1α activation in macrophages is critical for upregulation of profibrotic mediators and the development of liver fibrosis *in vivo*.

Methods

Animals: To selectively reduce HIF-1α or HIF-1β levels in myeloid cells HIF-1α$^{fl/fl}$ and HIF-1β$^{fl/fl}$ mice, described in detail previously (Tomita et al., 2000; Tomita et al., 2003), were crossed with mice expressing Cre recombinase under control of the lysozyme M promoter (LysMCre mice; Jackson Laboratories, Bar Harbor, ME) (Clausen et al., 1999). In these mice, Cre recombinase is expressed in monocytes, macrophages, and neutrophils (Clausen et al., 1999). Offspring of the HIF-1α$^{fl/fl}$ mouse breeding were HIF-1α$^{fl/fl}$-LysMCre+ (i.e., myeloid cells deficient in HIF-1α) or HIF-1α$^{fl/fl}$-LysMCre- (i.e., normal HIF-1α levels in myeloid cells). Offspring of the HIF-1β$^{fl/fl}$ mouse breeding were HIF-1β$^{fl/fl}$-LysMCre+ (i.e., myeloid cells deficient in HIF-1β) or HIF-1β$^{fl/fl}$-LysMCre- (i.e., normal HIF-1β levels in myeloid cells). PCR of genomic DNA was used to detect the floxed HIF-1α gene, floxed HIF-1β gene, and the Cre transgene as described previously (Tomita et al., 2000; Tomita et al., 2003; Copple et al., 2009).

All mice were maintained on a 12-h light/dark cycle under controlled temperature (18-21ºC) and humidity. Food (Rodent Chow; Harlan-Teklad, Madison, WI) and tap water were allowed *ad libitum*. All procedures on animals were carried out in accordance with the Guide for the Care and Use of Laboratory Animals promulgated by the National Institutes of Health.

Bile Duct Ligation (BDL): Mice were subjected to BDL as described previously (Kim et al., 2006). At 10 days after surgery, mice were anesthetized with sodium pentobarbital and euthanized by exsanguination.

Real-time Polymerase Chain Reaction (PCR): RNA was isolated using TRI reagent (Sigma Chemical Company), and contaminating DNA was removed using the TURBO DNA-free kit (Applied Biosystems, Foster City, CA). The RNA was then reverse transcribed into cDNA as described by us previously (Kim et al., 2006). Real-time PCR was performed on an Applied Biosystems 7900 Real-time PCR Instrument (Applied Biosystems) with the SYBR green DNA

PCR kit (Applied Biosystems). Real-time PCR was used to quantify mRNA levels on an Applied Biosystems Prism 7300 Real-time PCR Instrument (Applied Biosystems) using the SYBR green DNA PCR kit (Applied Biosystems) as described (Kim et al., 2006). Primer sequences for real-time PCR are shown in Table 1.

Kupffer Cell Isolation: Kupffer cells were isolated from mice and exposed to hypoxia as described by us previously (Copple et al., 2010).

Western Blot Analysis: Nuclear extracts were isolated from Kupffer cells as described previously (Copple et al., 2010). For western blot analysis, aliquots (15 μg) of nuclear extracts were subjected to 10% SDS-polyacrylamide gel electrophoresis, and proteins were transferred to Immobilon polyvinylidene difluoride transfer membranes (Millipore Corporation, Bedford, MA). The membranes were then probed with rabbit polyclonal anti-HIF-1α antibody (NB100-449, Novus Biologicals, Littleton, CO) diluted 1:1000 or mouse monoclonal anti-HIF-1β (Millipore) diluted 1:1000 followed by incubation with goat anti-rabbit antibody conjugated to horseradish peroxidase (Santa Cruz Biotechnology) for HIF-1α or goat anti-mouse antibody conjugated to horseradish peroxidase (Santa Cruz Biotechnology) for HIF-1β.

For TGF-β1 western blot, aliquots of liver extract (50 μg) were separated on a 10% SDS-polyacrylamide gel under non-denaturing conditions. TGF-β1 was detected using a monoclonal anti-TGF-β1 antibody (clone 9016; R&D Systems, Minneapolis, MN).

Assessment of Hepatic Injury and Serum Alkaline Phosphatase (ALP), Bilirubin, and Bile Acid Concentrations: Hepatocyte injury was evaluated by measuring the activity of alanine aminotransferase (ALT) (Pointe Scientific Inc., Canton, MI). Serum bile acid concentrations were determined by using a commercially available kit (Colorimetric Total Bile Acids Assay Kit; Bioquant, San Diego, CA). ALP and bilirubin were quantified in serum by using commercially available kits (Pointe Scientific Inc., Canton, MI).

Quantification of Type I Collagen, Cre Recombinase, Macrophages, and Neutrophils in the Liver: Type I collagen in the liver was detected using immunohistochemistry and quantified morphometrically by analyzing the area of immunohistochemical staining of type I collagen as described by us previously (Kim et al., 2006; Moon et al., 2009). An increase in the area of type I collagen staining in the liver is an indicator of fibrosis. Fluorescent staining in sections of liver was visualized on an Olympus BX41 microscope (Olympus, Lake Success, NY). For morphometric analysis of the total area of type I collagen in a liver section, digital images of 10, randomly chosen, low power (100X magnification) fields per tissue section were captured using an Olympus DP70 camera. Samples were coded such that the evaluator was not aware of the treatment, and the same exposure time was used for all captured images. Scion Image software (Scion Corporation, Frederick, MD) was then used to quantify the total area of type I collagen (number of positive pixels) using methods described in detail previously (Copple et al., 2002). The staining is expressed as a fraction of the total area. The 10 random fields analyzed for each liver section were averaged and counted as a replicate, i.e., each replicate represents a different mouse.

Neutrophils were detected in sections of liver and quantified as described previously (Kim et al., 2006).

For quantification of macrophages in the liver, sections of frozen liver were fixed in 4% formalin and then incubated with rat anti-mouse CD68 and rat anti-mouse F4/80 antibodies diluted 1:100 (AbD Serotec, Raleigh, NC). The sections were then incubated with goat anti-rat antibody conjugated with Alexa 488. The area of immunohistochemical staining was then quantified in sections of liver as described above for collagen quantification.

For detection of Cre recombinase in the liver, sections of frozen liver were fixed in 4% formalin and then incubated with rabbit anti-Cre recombinase antibody diluted 1:4000 (Imgenex,

San Diego, CA). The sections were then incubated with goat anti-rat antibody conjugated with Alexa 594.

Immunohistochemistry for PDGF-B in Sections of Mouse Liver: For PDGF-B immunostaining, livers were frozen in isopentane (Sigma Chemical Company) immersed in liquid nitrogen for 8 minutes. Sections of frozen liver were fixed in acetone for 10 minutes at -20°C. Sections were incubated with rabbit polyclonal anti-PDGF-B antibody (Bioworld Technology, Inc., St. Louis Park, MN) diluted 1:50 in PBS containing 3% goat serum at room temperature for 3 hours. The sections were washed with PBS, and then incubated with secondary antibody conjugated to Alexa 488 (green staining; Invitrogen). Macrophages were detected in the same sections as described above.

HIF-1α Immunohistochemistry in Sections of Human Liver: Research involving human livers was reviewed by the University of Kansas Medical Center Human Research Protection Program and the use of de-identified human liver samples was approved. The specimens used in this study were collected by and provided by the KU Liver Center Tissue Bank at The University of Kansas Medical Center. Diseased liver tissue utilized was from patients with primary biliary cirrhosis (2 Females, age 60, 61; 1 Male, age 47) and patients with primary sclerosing cholangitis (2 Males, age 45, 55; 1 Female, age 70). Control liver sections were obtained from liver tissue taken from donor livers prior to transplantation. 5 μm frozen sections were fixed for 10 minutes in 4% neutral-buffered formalin, washed with PBS, then blocked for 30 minutes in 10% goat serum. Sections were then incubated with primary antibodies, rabbit anti-human HIF-1α (NB100-134, Novus Biologicals, Littleton, CO) diluted 1:100 and mouse anti-human CD68 (Ab-3, Thermo Scientific, Fremont, CA) or mouse anti- human α-SMA (Chemicon, Temecula, CA) each diluted 1:100 overnight at 4 degrees. Sections were subsequently washed with PBS and then incubated with secondary Alexa594-conjugated rabbit anti-mouse and Alexa488-

conjuated goat anti-rabbit secondary antibodies, each diluted at 1:500 in block buffer for 1 hour at room temperature. Sections were washed with PBS, counterstained with DAPI.

Statistical Analysis: Results are presented as the mean ± SEM. Data were analyzed by Analysis of Variance (ANOVA). Data expressed as a fraction were transformed by arc sine square root prior to analysis. Comparisons among group means were made using the Student-Newman-Keuls test. The criterion for significance was $p < 0.05$ for all studies.

Results

HIF-1β Deletion in Myeloid Cells does not affect Liver Injury or Hepatic Inflammation after BDL. To determine whether HIF-1β in myeloid cells is critical for the development of liver fibrosis, HIF-1β$^{fl/fl}$ mice were crossed with LysMCre mice. To confirm that HIF-1β was deleted in hepatic macrophages (i.e., Kupffer cells), these cells were isolated from HIF-1βLysMCre – and HIF-1βLysMCre + mice, and HIF-1β was detected by western blot. HIF-1β was detected in Kupffer cells from HIF-1βLysMCre – mice but not in Kupffer cells from HIF-1βLysMCre + mice (Figure 1A). Next, to confirm that Cre recombinase was only expressed in macrophages in the liver, Cre recombinase was detected by immunohistochemistry in sections of liver from HIF-1βLysMCre + mice subjected to BDL (red staining, Figure 1B). Macrophages were then identified in the same section of liver by immunohistochemistry (green staining, Figure 1C). When Cre recombinase immunostaining and macrophage immunostaining were overlaid, Cre recombinase was only detected in hepatic macrophages (Figure 1D).

Next, HIF-1βLysMCre – and HIF-1βLysMCre + mice were subjected to BDL and liver injury and inflammation were assessed 10 days after surgery. ALT, bilirubin, ALP, and bile acids in serum were increased to a similar extent in HIF-1βLysMCre – mice and HIF-1βLysMCre + mice at 10 days after BDL (Table 2). In addition, the extent of necrosis was similar in these mice after BDL (Figures 2).

To evaluate the extent of hepatic inflammation after BDL, macrophages and neutrophils were detected in sections of liver by immunohistochemistry. In addition, levels of proinflammatory mediators were quantified by real-time PCR. Macrophage and neutrophil numbers were increased to a similar extent in the livers of HIF-1βLysMCre – and HIF-1βLysMCre + mice after BDL (Figure 3). In addition, upregulation of the chemokines,

keratinocyte-derived chemotactic factor (KC) and macrophage inflammatory protein-2 (MIP-2), and upregulation of the cytokine tumor necrosis factor-α (TNF-α) were unaffected by deficiency of HIF-1β in myeloid cells (Table 3).

HIF-1β Deletion in Myeloid Cells Reduces Liver Fibrosis after BDL. Next, we evaluated biomarkers of liver fibrosis to test the hypothesis that HIF activation in myeloid cells is required for the development of liver fibrosis after BDL. α-smooth muscle actin mRNA levels were increased to a greater extent in the livers of HIF-1βLysMCre – mice after BDL when compared to bile duct-ligated HIF-1βLysMCre + mice (Figure 4A). Type I collagen mRNA levels were increased in the livers of HIF-1βLysMCre – mice after BDL (Figure 4B). Type I collagen mRNA levels were significantly lower in HIF-1βLysMCre + mice after BDL (Figure 4B). Extensive deposition of type I collagen protein was observed in periportal regions of liver from HIF-1βLysMCre – mice after BDL (Figure 4C). Lower levels of type I collagen were observed in bile duct-ligated HIF-1βLysMCre + mice (Figure 4D). A significant reduction in hepatic type I collagen protein in these mice was confirmed by quantification of the area of immunohistochemical staining of type I collagen in sections of liver (Figure 4E). These data demonstrate that HIF signaling in myeloid cells is important for the development of liver fibrosis after BDL.

HIF-1β in Myeloid Cells is required for Upregulation of PDGF-B after BDL. Next we determined whether HIF-1β deficiency affected upregulation of mediators that are important for development of fibrosis, such as plasminogen activator inhibitor-1 (PAI-1), fibroblast growth factor-2 (FGF-2), platelet-derived growth factor-B (PDGF-B), monocyte chemotactic protein-1 (MCP-1), and transforming growth factor-β1 (TGF-β1). In addition, we determined the impact of HIF deficiency in myeloid cells on levels of proangiogenic mediators, including vascular

endothelial growth factor-A (VEGF-A), angiopoietin-1 (Ang-1), and Ang-2. PAI-1, FGF-2, PDGF-B, and MCP-1 mRNA levels were increased in HIF-1βLysMCre - mice after BDL (Table 4). PDGF-B and MCP-1 mRNA levels were significantly lower in HIF-1βLysMCre + after BDL when compared to HIF-1βLysMCre – mice (Table 4). In contrast, mRNA levels of VEGF-A, Ang-1, and Ang-2 were not significantly increased in the livers of either HIF-1βLysMCre – or HIF-1βLysMCre + after BDL (Table 4). To confirm this, we evaluated VEGF-A protein levels by western blot and immunohistochemistry. Consistent with VEGF-A mRNA levels, VEGF-A protein was not increased in the liver by 10 days after BDL (data not shown).

Levels of latent TGF-β1 protein (75 kD) and active TGF-β1 protein (25 kD) were increased to a similar extent in the livers of HIF-1βLysMCre – and HIF-1βLysMCre + mice after BDL (Figure 5). Consistent with this, the ratio of active TGF-β1 to latent TGF-β1 was not different between HIF-1βLysMCre – and HIF-1βLysMCre + mice after BDL (HIF-1βLysMCre –: 0.44 +/- 0.07 vs. HIF-1βLysMCre +: 0.53 +/- 0.05).

Since myeloid cell-specific HIF-1β deficiency largely prevented the increase in PDGF-B and MCP-1 mRNAs in the liver, we next evaluated whether PDGF-B and MCP-1 protein levels were increased in a HIF-1β-dependent manner. Immunohistochemistry was used to detect PDGF-B protein in hepatic macrophages. PDGF-B protein was not detected in livers from sham-operated mice (data not shown). PDGF-B protein levels were increased in the livers of HIF-1βLysMCre – mice after BDL (Figure 6B, green staining). Furthermore, PDGF-B protein (green staining) co-localized with hepatic macrophages (red staining) in these mice (Figure 6C). In contrast, PDGF-B protein was not detected in hepatic macrophages in HIF-1βLysMCre + mice after BDL (Figures 6D-6F). Next, serum concentrations of MCP-1 protein were quantified.

JPET Fast Forward. Published on January 23, 2012 as DOI: 10.1124/jpet.111.189340
This article has not been copyedited and formatted. The final version may differ from this version.

In contrast to MCP-1 mRNA levels (Table 4), MCP-1 protein concentrations were increased to a similar extent in HIF-1βLysMCre – and HIF-1βLysMCre + mice after BDL (Figure 6G)

HIF-1α in Myeloid Cells Contributes to the Development of Liver Fibrosis. During hypoxia, HIF-1β heterodimerizes with either HIF-1α or HIF-2α to regulate gene expression (Cash et al., 2007). Since our results above demonstrate a role for myeloid HIF-1β in liver fibrosis, we determined whether HIF-1α contributed to liver fibrosis and upregulation of profibrotic genes. To determine the role of HIF-1α in myeloid cells, HIF-$1\alpha^{fl/fl}$ mice were crossed with LysMCre mice. Kupffer cells were isolated from HIF-1αLysMCre – mice and HIF-1αLysMCre + mice and exposed to 1% oxygen, a concentration of oxygen that stimulates nuclear accumulation of HIF-1α in these cells (Copple et al., 2010). HIF-1α protein was detected in nuclear extracts from Kupffer cells isolated from HIF-1αLysMCre – mice (Figure 7A). HIF-1α protein levels were substantially lower in hypoxic Kupffer cells isolated from HIF-1αLysMCre + mice (Figure 7A).

ALT activity was increased to a similar extent in HIF-1αLysMCre – and HIF-1αLysMCre + after BDL (Figure 7B). In addition, pathological changes that occurred in the liver were similar (Figures 7C and 7D). mRNA levels of α-smooth muscle actin, type I collagen, and PDGF-B were increased in HIF-1αLysMCre- mice after BDL (Figure 8). mRNA levels of all of these genes were significantly lower in bile duct-ligated HIF-1αLysMCre + mice (Figure 8).

Activation of HIF-1α in Macrophages, Hepatocytes, and Fibroblasts in Livers of Patients with Primary Biliary Cirrhosis (PBC) and Primary Sclerosing Cholangitis (PSC). Immunohistochemistry was used to detect HIF-1α in macrophages and fibroblasts in livers from three patients with PBC, 3 patients with PSC, and 3 normal human livers. Nuclear accumulation

of HIF-1α was observed in macrophages in the liver of a patient with PBC (Figure 9A). In addition, nuclear HIF-1α was observed in hepatocytes adjacent to HIF-1α-positive macrophages (Figure 9A). HIF-1α was detected in macrophages in livers from all three patients with PBC. Similarly, nuclear HIF-1α was observed in macrophages in all livers from patients with PSC (Figure 9C). In contrast, HIF-1α protein was not detected in the nuclei of macrophages in normal human livers (Figure 9E). We also observed nuclear HIF-1α protein in cells within fibrotic regions of liver from patients with PBC and PSC; therefore, we determined whether fibroblasts, identified by α-SMA immunostaining, were positive for HIF-1α. As shown in Figure 9G, HIF-1α protein was detected in the nuclei of α-SMA-positive cells in all livers from patients with PBC and PSC. In addition, HIF-1α protein was detected in the nuclei of hepatocytes adjacent to regions of bridging fibrosis (Figure 9G).

Discussion

Our results demonstrate that HIF-1β and HIF-1α in myeloid cells contribute to the development of liver fibrosis after BDL. In LysMCre mice, Cre recombinase is expressed in macrophages and neutrophils (Clausen et al., 1999). Accordingly, it is possible that HIF-1β and HIF-1α deletion in macrophages and/or neutrophils was responsible for the reduction of fibrosis observed in our studies. A recent study showed, however, that neutrophil depletion does not affect development of liver fibrosis after BDL (Saito et al., 2003). Accordingly, it is unlikely that HIF activation in neutrophils contributes to the development of fibrosis after BDL. Therefore, our results indicate HIF-1β and HIF-1α in macrophages is important for liver fibrosis.

The mechanism by which activation of HIFs in macrophages promoted fibrosis may be in part due to HIF-dependent production of PDGF-B by hepatic macrophages during chronic injury. PDGF-B is a potent mitogen and chemotaxin for hepatic stellate cells (Friedman and Arthur, 1989; Carloni et al., 1997; Marra et al., 1997). Furthermore, PDGF-B increases expression of α-SMA in peribiliary fibroblasts, and inhibition of PDGF-B signaling reduces fibrosis after BDL (Kinnman et al., 2003). Consistent with our results (Figure 6), others have demonstrated that hepatic macrophages express PDGF-B in the liver during chronic injury (Pinzani et al., 1996). The mechanism by which chronic injury increases expression of PDGF-B in hepatic macrophages, however, has remained largely unknown. We previously demonstrated that HIF-1α is activated in hepatic macrophages after BDL (Moon et al., 2009). We also demonstrated that exposure of Kupffer cells *in vitro* to hypoxia upregulates PDGF-B in a HIF-1α-dependent manner (Copple et al., 2010). Collectively, these studies suggested that HIF-1α may be an important regulator of PDGF-B in the liver during the development of fibrosis. Consistent with this, our present study demonstrated that deletion of either HIF-1α or HIF-1β in myeloid cells

attenuated the increase in PDGF-B mRNA (Table 4 and Figure 8) and prevented the increase in PDGF-B protein in hepatic macrophages during the development of fibrosis in BDL mice (Figure 6). This was associated with a marked reduction in α-SMA and type I collagen (Figures 4 and 8). HIF-1β deletion did not affect hepatic macrophage accumulation (Figure 3), indicating that the decrease in PDGF-B was not simply due to a reduction in the numbers of hepatic macrophages. It is likely that HIF-1α and HIF-1β directly regulate PDGF-B in macrophages, as studies have shown that these HIFs directly regulate this gene in other cells types (Yoshida et al., 2006). Collectively, this suggests that during chronic injury induced by cholestasis, hepatic macrophages accumulate in hypoxic regions of liver where hypoxia stimulates activation of HIF-1α. HIF-1α then heterodimerizes with HIF-1β and regulates production of PDGF-B that promotes fibrosis. Of importance to human disease, our studies demonstrated further that HIF-1α is activated in hepatic macrophages in PBC and PSC patients with fibrosis (Figure 9), suggesting that this mechanism may also be important for regulation of PDGF-B and the progression of fibrosis in humans with cholestatic liver disease.

An interesting observation from these studies is that although deficiency of either HIF-1α or HIF-1β in myeloid cells reduced liver fibrosis after BDL, it did not affect hepatocyte injury. This suggests that liver fibrosis after BDL is not dependent upon hepatocyte injury. Consistent with this observation, we demonstrated previously that early growth response factor-1 knockout mice had reduced liver injury and neutrophil accumulation after BDL when compared to wild-type mice, but had similar levels of fibrosis (Kim et al., 2006). Similarly, Fickert and colleagues demonstrated that FXR knockout mice have reduced liver fibrosis after BDL but have similar levels of liver injury when compared to wild-type mice (Fickert et al., 2009). Collectively, these studies indicate that hepatocyte injury after BDL is not an important stimulus for hepatic fibrosis. It remains possible, however, that HIFs may contribute to the development of liver injury at

earlier times after BDL. Our study focused on a late time-point after BDL (i.e., 10 days). Much of the liver injury after BDL occurs within the first few days and it is possible that deletion of HIFs delayed the development of liver injury. This may have been sufficient to delay the development of liver fibrosis. Further studies are needed to evaluate this possibility, however.

Studies indicate that angiogenesis is important for the development of hepatic fibrosis (Rosmorduc et al., 1999; Corpechot et al., 2002; Taura et al., 2008). Furthermore, a key function of HIFs is to regulate production of pro-angiogenic mediators (Forsythe et al., 1996; Kelly et al., 2003; Yamakawa et al., 2003). Surprisingly, however, although HIF-1α was activated in the liver after BDL, levels of pro-angiogenic mediators, such as VEGF-A and angiopoietins, remained unchanged. We reported previously that hypoxia increases expression of VEGF-A in primary mouse hepatocytes, Kupffer cells, and hepatic stellate cells in a HIF-1α-dependent manner (Copple et al., 2009; Copple et al., 2010; Copple et al., 2011), demonstrating that HIF-1α regulates production of these mediators in these cells types. One possible explanation for the lack of induction of pro-angiogenic mediators may be that they are transiently produced and the time-point we chose did not coincide with upregulation of VEGF-A and angiopoietins. In addition, it is possible that upregulation of VEGF-A occurs at a later time-point in this model. Consistent with this, it was shown previously that upregulation of VEGF in the livers of rats after BDL required several weeks (Rosmorduc et al., 1999).

In addition to detecting nuclear HIF-1α protein in macrophages in the livers of patients with PBC and PSC, we also detected nuclear HIF-1α protein in α-SMA positive cells (Figure 9). We recently demonstrated that exposure of primary mouse hepatic stellate cells to hypoxia increased expression of a number of genes involved in the genesis of liver fibrosis, including the chemokine receptors Ccr1 and Ccr5, prolyl-4-hydroxylase α1, prolyl-4-hydroxylase α2, and the

proangiogenic mediators, placental growth factor and angiopoietin-like 4 (Copple et al., 2011). Many of these were increased in hepatic stellate cells in a HIF-dependent manner (Copple et al., 2011). Accordingly, it is possible that in addition to macrophages, activation of HIF-1α in hepatic stellate cells may be important for the development of liver fibrosis.

Collectively, these studies demonstrate that HIF-1α and HIF-1β are important regulators of profibrotic mediator production by macrophages during the development of liver fibrosis in cholestatic mice. Furthermore, these studies indicate that this mechanism may be important for fibrosis development in humans as HIF-1α was activated in macrophages in the livers of patients with PBC and PSC. Accordingly, these studies suggest that therapeutic targeting of HIF-1α may be effective at preventing the progression of liver fibrosis in patients with cholestatic liver disease and potentially in patients with liver fibrosis produced by other hepatic insults.

Acknowledgements

The authors wish to acknowledge James P. Luyendyk, Ph.D. for critical reading of the manuscript. The authors wish to think Erik Schadde, M.D, Richard Gilroy, M.D., Bashar Abdulkarim, M.D., Ph.D, Jameson Forster,M.D, Mojtaba Olyaee, M.D., and Atta M Nawabi, M.D. for assistance in collecting human liver specimens utilized in this study. The authors wish to thank Natali Navarro-Cazarez, Marsha Danley, Yvonne Wan, Ph.D., and Dr. Ossama Tawfik for help with procuring and preparation of frozen liver sections.

Authorship Contributions

Participated in research design: BLC, SK, CW

Conducted experiments: BLC, SK, CW

Performed data analysis: BLC, CW

Wrote or contributed to the writing of the manuscript: BLC, SK

References

Carloni V, Romanelli RG, Pinzani M, Laffi G and Gentilini P (1997) Focal adhesion kinase and phospholipase C gamma involvement in adhesion and migration of human hepatic stellate cells. *Gastroenterology* **112**:522-531.

Cash TP, Pan Y and Simon MC (2007) Reactive oxygen species and cellular oxygen sensing. *Free Radic Biol Med* **43**:1219-1225.

Clausen BE, Burkhardt C, Reith W, Renkawitz R and Forster I (1999) Conditional gene targeting in macrophages and granulocytes using LysMcre mice. *Transgenic research* **8**:265-277.

Coleman ML and Ratcliffe PJ (2007) Oxygen sensing and hypoxia-induced responses. *Essays Biochem* **43**:1-15.

Copple BL, Bai S, Burgoon LD and Moon JO (2011) Hypoxia-inducible factor-1alpha regulates the expression of genes in hypoxic hepatic stellate cells important for collagen deposition and angiogenesis. *Liver Int* **31**:230-244.

Copple BL, Bai S and Moon JO (2010) Hypoxia-inducible factor-dependent production of profibrotic mediators by hypoxic Kupffer cells. *Hepatol Res* **40**:530-539.

Copple BL, Banes A, Ganey PE and Roth RA (2002) Endothelial cell injury and fibrin deposition in rat liver after monocrotaline exposure. *Toxicol Sci* **65**:309-318.

Copple BL, Bustamante JJ, Welch TP, Kim ND and Moon JO (2009) Hypoxia-inducible factor-dependent production of profibrotic mediators by hypoxic hepatocytes. *Liver Int* **29**:1010-1021.

Copple BL, Rondelli CM, Maddox JF, Hoglen NC, Ganey PE and Roth RA (2004) Modes of cell death in rat liver after monocrotaline exposure. *Toxicol Sci* **77**:172-182.

Corpechot C, Barbu V, Wendum D, Kinnman N, Rey C, Poupon R, Housset C and Rosmorduc O (2002) Hypoxia-induced VEGF and collagen I expressions are associated with angiogenesis and fibrogenesis in experimental cirrhosis. *Hepatology* **35**:1010-1021.

Duffield JS, Forbes SJ, Constandinou CM, Clay S, Partolina M, Vuthoori S, Wu S, Lang R and Iredale JP (2005) Selective depletion of macrophages reveals distinct, opposing roles during liver injury and repair. *J Clin Invest* **115**:56-65.

Faiz Kabir Uddin Ahmed A, Ohtani H, Nio M, Funaki N, Iwami D, Kumagai S, Sato E, Nagura H and Ohi R (2000) In situ expression of fibrogenic growth factors and their receptors in biliary atresia: comparison between early and late stages. *The Journal of pathology* **192**:73-80.

Fausto N (2000) Liver regeneration. *J Hepatol* **32**:19-31.

Fickert P, Fuchsbichler A, Moustafa T, Wagner M, Zollner G, Halilbasic E, Stoger U, Arrese M, Pizarro M, Solis N, Carrasco G, Caligiuri A, Sombetzki M, Reisinger E, Tsybrovskyy O, Zatloukal K, Denk H, Jaeschke H, Pinzani M and Trauner M (2009) Farnesoid X receptor critically determines the fibrotic response in mice but is expressed to a low extent in human hepatic stellate cells and periductal myofibroblasts. *Am J Pathol* **175**:2392-2405.

Forsythe JA, Jiang BH, Iyer NV, Agani F, Leung SW, Koos RD and Semenza GL (1996) Activation of vascular endothelial growth factor gene transcription by hypoxia-inducible factor 1. *Mol Cell Biol* **16**:4604-4613.

Friedman SL (2008) Mechanisms of hepatic fibrogenesis. *Gastroenterology* **134**:1655-1669.

Friedman SL and Arthur MJ (1989) Activation of cultured rat hepatic lipocytes by Kupffer cell conditioned medium. Direct enhancement of matrix synthesis and stimulation of cell proliferation via induction of platelet-derived growth factor receptors. *J Clin Invest* **84**:1780-1785.

Gaber T, Dziurla R, Tripmacher R, Burmester GR and Buttgereit F (2005) Hypoxia inducible factor (HIF) in rheumatology: low O2! See what HIF can do! *Ann Rheum Dis* **64**:971-980.

Ji S, Lemasters JJ, Christenson V and Thurman RG (1982) Periportal and pericentral pyridine nucleotide fluorescence from the surface of the perfused liver: evaluation of the hypothesis that chronic treatment with ethanol produces pericentral hypoxia. *Proc Natl Acad Sci U S A* **79**:5415-5419.

Kelly BD, Hackett SF, Hirota K, Oshima Y, Cai Z, Berg-Dixon S, Rowan A, Yan Z, Campochiaro PA and Semenza GL (2003) Cell type-specific regulation of angiogenic growth factor gene expression and induction of angiogenesis in nonischemic tissue by a constitutively active form of hypoxia-inducible factor 1. *Circulation research* **93**:1074-1081.

Kim ND, Moon JO, Slitt AL and Copple BL (2006) Early growth response factor-1 is critical for cholestatic liver injury. *Toxicol Sci* **90**:586-595.

Kinnman N, Francoz C, Barbu V, Wendum D, Rey C, Hultcrantz R, Poupon R and Housset C (2003) The myofibroblastic conversion of peribiliary fibrogenic cells distinct from hepatic stellate cells is stimulated by platelet-derived growth factor during liver fibrogenesis. *Lab Invest* **83**:163-173.

Marra F, Gentilini A, Pinzani M, Choudhury GG, Parola M, Herbst H, Dianzani MU, Laffi G, Abboud HE and Gentilini P (1997) Phosphatidylinositol 3-kinase is required for platelet-derived growth factor's actions on hepatic stellate cells. *Gastroenterology* **112**:1297-1306.

Moon JO, Welch TP, Gonzalez FJ and Copple BL (2009) Reduced liver fibrosis in hypoxia-inducible factor-1alpha-deficient mice. *Am J Physiol Gastrointest Liver Physiol* **296**:G582-592.

Nakatsukasa H, Nagy P, Evarts RP, Hsia CC, Marsden E and Thorgeirsson SS (1990) Cellular distribution of transforming growth factor-beta 1 and procollagen types I, III, and IV transcripts in carbon tetrachloride-induced rat liver fibrosis. *J Clin Invest* **85**:1833-1843.

Pinzani M, Milani S, Herbst H, DeFranco R, Grappone C, Gentilini A, Caligiuri A, Pellegrini G, Ngo DV, Romanelli RG and Gentilini P (1996) Expression of platelet-derived growth factor and its receptors in normal human liver and during active hepatic fibrogenesis. *Am J Pathol* **148**:785-800.

Rivera CA, Bradford BU, Hunt KJ, Adachi Y, Schrum LW, Koop DR, Burchardt ER, Rippe RA and Thurman RG (2001) Attenuation of CCl(4)-induced hepatic fibrosis by GdCl(3) treatment or dietary glycine. *Am J Physiol Gastrointest Liver Physiol* **281**:G200-207.

Rosmorduc O and Housset C (2010) Hypoxia: a link between fibrogenesis, angiogenesis, and carcinogenesis in liver disease. *Seminars in liver disease* **30**:258-270.

Rosmorduc O, Wendum D, Corpechot C, Galy B, Sebbagh N, Raleigh J, Housset C and Poupon R (1999) Hepatocellular hypoxia-induced vascular endothelial growth factor expression and angiogenesis in experimental biliary cirrhosis. *Am J Pathol* **155**:1065-1073.

Saito JM, Bostick MK, Campe CB, Xu J and Maher JJ (2003) Infiltrating neutrophils in bile duct-ligated livers do not promote hepatic fibrosis. *Hepatol Res* **25**:180-191.

Semenza GL and Wang GL (1992) A nuclear factor induced by hypoxia via de novo protein synthesis binds to the human erythropoietin gene enhancer at a site required for transcriptional activation. *Mol Cell Biol* **12**:5447-5454.

Taura K, De Minicis S, Seki E, Hatano E, Iwaisako K, Osterreicher CH, Kodama Y, Miura K, Ikai I, Uemoto S and Brenner DA (2008) Hepatic stellate cells secrete angiopoietin 1 that induces angiogenesis in liver fibrosis. *Gastroenterology* **135**:1729-1738.

Tomita S, Sinal CJ, Yim SH and Gonzalez FJ (2000) Conditional disruption of the aryl hydrocarbon receptor nuclear translocator (Arnt) gene leads to loss of target gene induction by the aryl hydrocarbon receptor and hypoxia-inducible factor 1alpha. *Molecular endocrinology (Baltimore, Md* **14**:1674-1681.

Tomita S, Ueno M, Sakamoto M, Kitahama Y, Ueki M, Maekawa N, Sakamoto H, Gassmann M, Kageyama R, Ueda N, Gonzalez FJ and Takahama Y (2003) Defective brain development in mice lacking the Hif-1alpha gene in neural cells. *Mol Cell Biol* **23**:6739-6749.

Yamakawa M, Liu LX, Date T, Belanger AJ, Vincent KA, Akita GY, Kuriyama T, Cheng SH, Gregory RJ and Jiang C (2003) Hypoxia-inducible factor-1 mediates activation of cultured vascular endothelial cells by inducing multiple angiogenic factors. *Circulation research* **93**:664-673.

Yoshida D, Kim K, Noha M and Teramoto A (2006) Hypoxia inducible factor 1-alpha regulates of platelet derived growth factor-B in human glioblastoma cells. *J Neurooncol* **76**:13-21.

Footnotes

This study was supported by the National Institutes of Health National Institute of Diabetes and Digestive and Kidney Disease [Grant DK073566] and National Institutes of Health COBRE (Center of Biomedical Research Excellence) [Grant P20 RR021940] as well as the Molecular Biology Core and the Histology Core supported by the COBRE grant. In addition, this work was supported by the National Institutes of Health National Center for Research Resources [Grant P20 RR016475].

Author to receive reprint requests:

Bryan L. Copple

Department of Pharmacology & Toxicology

Michigan State University

B403 Life Sciences Building

East Lansing, MI 48823

Phone: (517)884-6691

Fax: (517)353-8915

E-mail: copple@msu.edu

JPET Fast Forward. Published on January 23, 2012 as DOI: 10.1124/jpet.111.189340
This article has not been copyedited and formatted. The final version may differ from this version.

Figure Legends

Figure 1. Decreased HIF-1β protein in Kupffer cells isolated from HIF-1βLysMCre + mice. (A) Kupffer cells were isolated from HIF-1βLysMCre – and HIF-1βLysMCre + mice, and HIF-1β was detected by western blot. HIF-1βLysMCre + mice were subjected to BDL. Ten days after surgery, immunohistochemistry was used to detect Cre recombinase (red staining in B and D) and macrophages (green staining in C and D). B, C, and D show the same field. Yellow staining in D demonstrates colocalization of Cre recombinase and macrophages. Bar = 50 μm.

Figure 2. Liver injury in HIF-1βLysMCre – and HIF-1βLysMCre + mice after BDL. HIF-1βLysMCre – and HIF-1βLysMCre + mice were subjected to sham operation or BDL. Ten days after surgery, sections of liver were stained with hematoxylin and eosin. Representative photomicrographs from (A) HIF-1βLysMCre – and (B) HIF-1βLysMCre + mice subjected to BDL. Arrows indicate areas of necrosis. PP: periportal. Bar = 50 μm.

Figure 3. Levels of macrophages and neutrophils in HIF-1βLysMCre – and HIF-1βLysMCre + mice after BDL. HIF-1βLysMCre – and HIF-1βLysMCre + mice were subjected to sham operation or BDL. Ten days after surgery, macrophages and neutrophils were detected in livers by immunohistochemistry. Representative photomicrographs of immunohistochemistry for macrophages in liver sections from (A) HIF-1βLysMCre – and (B) HIF-1βLysMCre + mice subjected to BDL. Positive staining appears black in the photomicrographs. Bar = 100 μm. (C) The area of macrophage immunostaining was quantified using morphometric techniques. (D) Neutrophils were quantified in sections of liver. Data are expressed as mean +/- SEM; n=8. [a]Significantly different ($p < 0.05$) from sham-operated mice.

JPET Fast Forward. Published on January 23, 2012 as DOI: 10.1124/jpet.111.189340
This article has not been copyedited and formatted. The final version may differ from this version.

Figure 4. Liver Fibrosis in HIF-1βLysMCre – and HIF-1βLysMCre + mice after BDL. HIF-1βLysMCre – and HIF-1βLysMCre + mice were subjected to sham operation or BDL. Ten days after surgery, mRNA levels of (A) α-smooth muscle actin (B) type I collagen were quantified by real-time PCR. Representative photomicrographs of type I collagen immunohistochemistry in liver sections from bile duct-ligated (C) HIF-1βLysMCre – and (D) HIF-1βLysMCre + mice. Positive staining appears dark grey in the photomicrographs. PP: periportal. Bar = 50 μm. (E) The area of type I collagen immunostaining was quantified in sections of liver. Data are expressed as mean +/- SEM; n=8. [a]Significantly different ($p < 0.05$) from sham-operated mice. [b]Significantly different ($p < 0.05$) from bile duct-ligated HIF-1βLysMCre – mice.

Figure 5. TGF-β1 protein levels in livers of HIF-1βLysMCre – and HIF-1βLysMCre + mice after BDL. HIF-1βLysMCre – and HIF-1βLysMCre + mice were subjected to sham operation or BDL. Ten days after surgery, western blot was used to detect TGF-β1 in liver homogenates.

Figure 6. Quantification of PDGF-B and MCP-1 protein in HIF-1βLysMCre – and HIF-1βLysMCre + mice after BDL. HIF-1βLysMCre – and HIF-1βLysMCre + mice were subjected to sham operation or BDL. Ten days after surgery, immunohistochemistry was used to detect macrophages (red staining in A, C, D, and F) and PDGF-B (green staining in B, C, E, and F) in livers sections from HIF-1βLysMCre – (A, B, and C) and HIF-1βLysMCre + (D, E, and F) mice subjected to BDL. A, B, and C show the same field. D, E, and F show the same field. Arrows indicate PDGF-B positive macrophages in HIF-1βLysMCre –. Dashed arrows indicate macrophages negative for PDGF-B in HIF-1βLysMCre +. (G) MCP-1 protein was quantified in

serum. Data are expressed as mean +/- SEM; n=8. [a]Significantly different ($p < 0.05$) from sham-operated mice.

Figure 7. Liver injury in HIF-1αLysMCre – and HIF-1αLysMCre + mice after BDL. (A) Kupffer cells were isolated from HIF-1αLysMCre – and HIF-1αLysMCre + mice and exposed to 1% oxygen for 1 hour. HIF-1α was detected in nuclear extracts by western blot. HIF-1αLysMCre – and HIF-1αLysMCre + mice were subjected to sham operation or BDL. Ten days after surgery, (B) ALT activity was measured in serum. Data are expressed as mean +/- SEM; n=8. [a]Significantly different ($p < 0.05$) from sham-operated mice. Representative photomicrographs from (C) HIF-1αLysMCre – and (D) HIF-1αLysMCre + mice subjected to BDL. Arrows indicates area of necrosis. PP: periportal. Bar = 50 μm.

Figure 8. Liver fibrosis in HIF-1αLysMCre – and HIF-1αLysMCre + mice after BDL. HIF-1αLysMCre – and HIF-1αLysMCre + mice were subjected to sham operation or BDL. Ten days after surgery, mRNA levels of (A) α-smooth muscle actin, (B) type I collagen, and (C) PDGF-B were quantified by real-time PCR. Data are expressed as mean +/- SEM; n=8. [a]Significantly different ($p < 0.05$) from sham-operated mice. [b]Significantly different ($p < 0.05$) from bile duct-ligated HIF-1αLysMCre – mice.

Figure 9. HIF-1α activation in the livers of patients with PBC and PSC. Sections of frozen liver from patients with PBC (A, B, G, and H), patients with PSC (C and D), and normal human livers (E and F) were stained for HIF-1α (green staining in A, C, E and G) and either CD68 (red staining in A-F) or α-SMA (red staining in G and H). Nuclei were stained with DAPI (blue staining in B, D, F, and H). The same fields in A, C, E, and G are shown in B, D, F, and H. Insets show higher power fields. Arrows indicate HIF-1α positive nuclei in macrophages (A and

C) or α-SMA-positive cells (G). Arrowheads indicate HIF-1α positive nuclei in hepatocytes. Dashed arrows indicate macrophages negative for HIF-1α (E and F).

JPET Fast Forward. Published on January 23, 2012 as DOI: 10.1124/jpet.111.189340
This article has not been copyedited and formatted. The final version may differ from this version.

Table 1: Primer Sequences from Real-time PCR Analysis

Gene Name	Forward Primer	Reverse Primer
18S	5'-TTGACGGAAGGGCACCACCAG-3'	5'-GCACCACCACCCACGGAATCG-3'
α-Smooth Muscle Actin (α-SMA)	5'-CCACCGCAAATGCTTCTAAGT-3'	5'-GGCAGGAATGATTTGGAAAGG-3'
Collagen Type Iα1	5'-TGTGTTCCCTACTCAGCCGTCT-3'	5'-CATCGGTCATGCTCTCTCCAA-3'
Monocyte Chemotactic Protein-1 (MCP-1)	5'-ACATTCGGCGGTTGCTCTAGA-3'	5'-ACATCCTGTATCCACACGGCAG-3'
Plasminogen Activator Inhibitor-1 (PAI-1)	5'-AGTCTTTCCGACCAAGAGCA-3'	5'-ATCACTTGCCCCATGAAGAG-3'
Platelet-derived Growth Factor-B (PDGF-B)	5'-CCCACAGTGGCTTTTCATTT-3'	5'-GTGGAGGAGCAGACTGAAGG-3'
Fibroblast Growth Factor-2 (FGF-2)	5'-AGCGACCCACACGTCAAACTAC-3'	5'-CAGCCGTCCATCTTCCTTCATA-3'
Keratinocyte-derived Chemotactic Factor (KC)	5'-TGGCTGGGATTCACCTCAAG-3'	5'-GTGGCTATGACTTCGGTTTGG-3'
Macrophage Inflammatory Protein-2 (MIP-2)	5'-CTTTGGTTCTTCCGTTGAGG-3'	5'-CAAAAAGTTTGCCTTGACCC-3'
Tumor Necrosis Factor-α (TNF-α)	5'-GACCCTCACACTCAGATCATCTTCT-3'	5'-CCTCCACTTGGTGGTTTGCT-3'
Vascular Endothelial Growth Factor-A (VEGF-A)	5'-CATCTTCAAGCCGTCCTGTGT-3'	5'-CTCCAGGGCTTCATCGTTACA-3'
Angiopoietin-1 (Ang-1)	5'-TTTGCATTCTTCGCTGCCA-3'	5'-GGCACATTGCCCATGTTGA-3'
Ang-2	5'-ACCTTCAGAGACTGTGCGGAAA-3'	5'-CGTCCATGTCACAGTAGGCCTT-3'

JPET Fast Forward. Published on January 23, 2012 as DOI: 10.1124/jpet.111.189340
This article has not been copyedited and formatted. The final version may differ from this version.

Table 2: Serum biomarkers of liver injury and cholestasis in HIF-1βLysMCre – and HIF-1βLysMCre + mice after BDL.

	Sham Operation		Bile Duct Ligation	
Biomarker	**HIF-1β LysMCre -**	**HIF-1β LysMCre +**	**HIF-1β LysMCre -**	**HIF-1β LysMCre +**
ALT (U/L)	5.6 +/- 0.9	22.0 +/- 17.6	470.3 +/- 62.1[a]	463.9 +/- 71.6[a]
Bilirubin (mg/dl)	0.2 +/- 0.1	0.1 +/- 0.1	15.0 +/- 3.4[a]	15.9 +/- 3.6[a]
ALP (U/L)	124.2 +/- 9.8	123.1 +/- 11.6	846.0 +/- 261.5[a]	970.8 +/- 381.1[a]
Bile Acids (μM)	5.6 +/- 0.9	22.0 +/- 17.6	428.9 +/- 25.3[a]	414.6 +/- 31.8[a]

HIF-1βLysMCre – and HIF-1βLysMCre + mice were subjected to sham operation or BDL. Ten days after surgery, ALT activity, bilirubin concentrations, ALP activity, and bile acid concentrations were quantified in serum. Data are expressed as mean +/- SEM; n=8. [a]Significantly different (p < 0.05) from sham-operated mice.

JPET Fast Forward. Published on January 23, 2012 as DOI: 10.1124/jpet.111.189340
This article has not been copyedited and formatted. The final version may differ from this version.

Table 3: mRNA Levels of Proinflammatory Mediators in HIF-1βLysMCre – and HIF-1βLysMCre + mice after BDL.

	Sham Operation		Bile Duct Ligation	
Gene Name/ Function	**HIF-1β LysMCre -**	**HIF-1β LysMCre +**	**HIF-1β LysMCre -**	**HIF-1β LysMCre +**
KC	1.0 +/- 0.2	2.4 +/- 1.0	8.3 +/- 1.9[a]	8.2 +/- 0.8[a]
MIP-2	1.0 +/- 0.3	2.9 +/- 1.1	14.2 +/- 0.3[a]	20.6 +/- 0.3[a]
TNF-α	1.2 +/- 0.6	1.2 +/- 0.4	4.7 +/- 1.0[a]	3.4 +/- 0.7[a]

HIF-1βLysMCre – and HIF-1βLysMCre + mice were subjected to sham operation or BDL. Ten days after surgery, mRNA levels were quantified by real-time PCR. Data are expressed as mean +/- SEM; n=8. [a]Significantly different ($p < 0.05$) from sham-operated mice.

Table 4: mRNA Levels of Profibrotic and Proangiogenic Mediators in HIF-1βLysMCre – and HIF-1βLysMCre + mice after BDL.

	Sham Operation		Bile Duct Ligation	
Gene Name/ Function	**HIF-1β LysMCre -**	**HIF-1β LysMCre +**	**HIF-1β LysMCre -**	**HIF-1β LysMCre +**
PAI-1	1.5 +/- 1.0	1.5 +/- 1.0	148.1 +/- 56.0[a]	174.4 +/- 43.9[a]
FGF-2	1.0 +/- 0.1	0.7 +/- 0.1	3.7 +/- 1.6[a]	1.5 +/- 0.3
PDGF-B	1.0 +/- 0.1	1.0 +/- 0.8	14.5 +/- 0.3[a]	4.7 +/- 0.4[a,b]
MCP-1	1.0 +/- 1.3	1.0 +/- 1.7	12.3 +/- 0.3[a]	3.8 +/- 0.6[a,b]
VEGF-A	1.0 +/- 0.1	0.7 +/- 0.05[a]	0.4 +/- 0.01[a]	0.4 +/- 0.02[a]
Angiopoietin-1	1.0 +/- 0.1	1.9 +/- 1.1	1.0 +/- 0.1	1.0 +/- 0.1
Angiopoietin-2	1.0 +/- 0.2	0.7 +/- 0.2	1.6 +/- 0.4	1.4 +/- 0.3

HIF-1βLysMCre – and HIF-1βLysMCre + mice were subjected to sham operation or BDL. Ten days after surgery, mRNA levels were quantified by real-time PCR. Data are expressed as mean +/- SEM; n=8. [a]Significantly different ($p < 0.05$) from sham-operated mice. [b]Significantly different ($p < 0.05$) from bile duct-ligated HIF-1βLysMCre – mice.

Figure 1

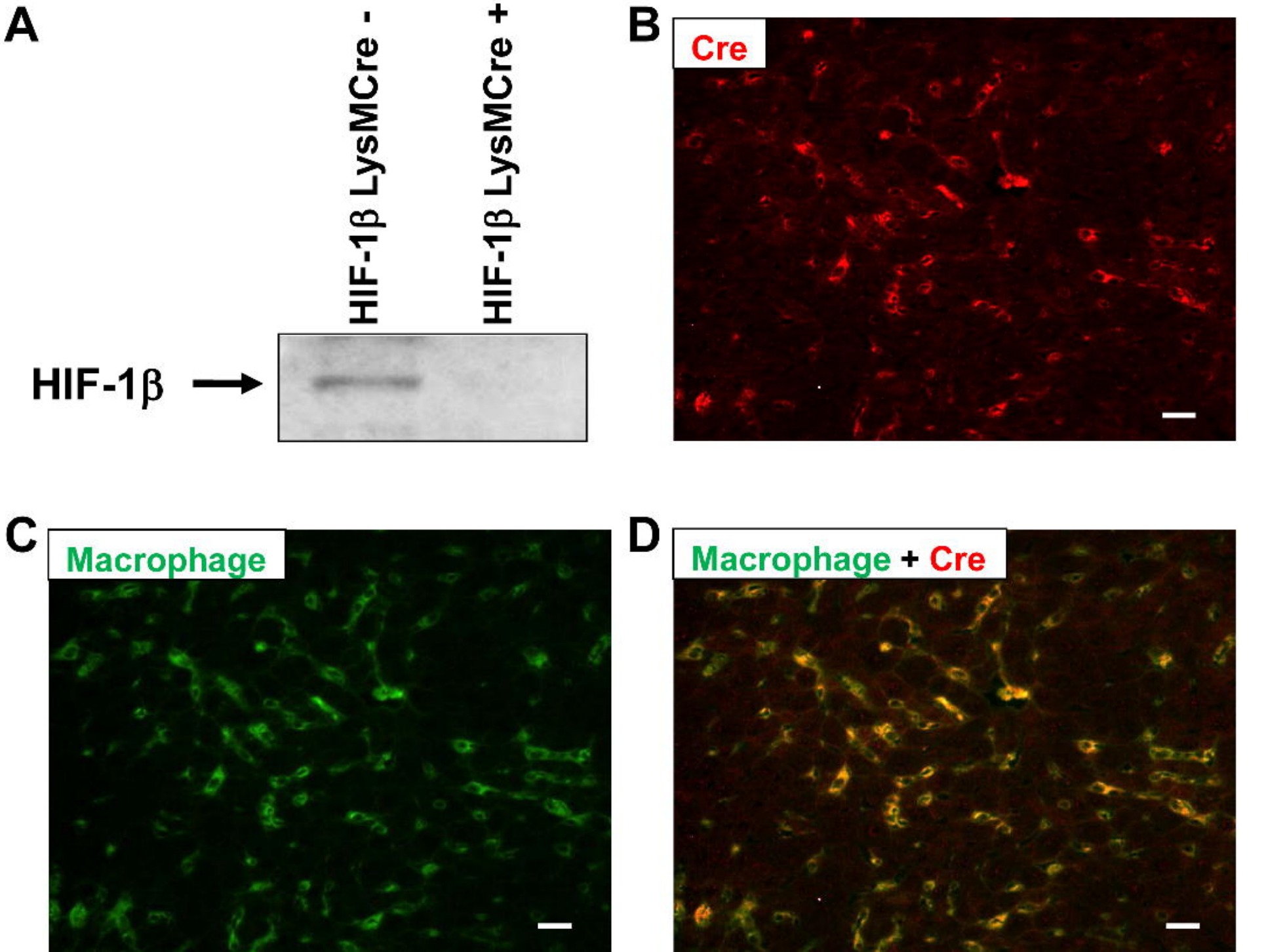
A
HIF-1β LysMCre -
HIF-1β LysMCre +
HIF-1β
B
Cre
C
Macrophage
D
Macrophage + Cre

Figure 2

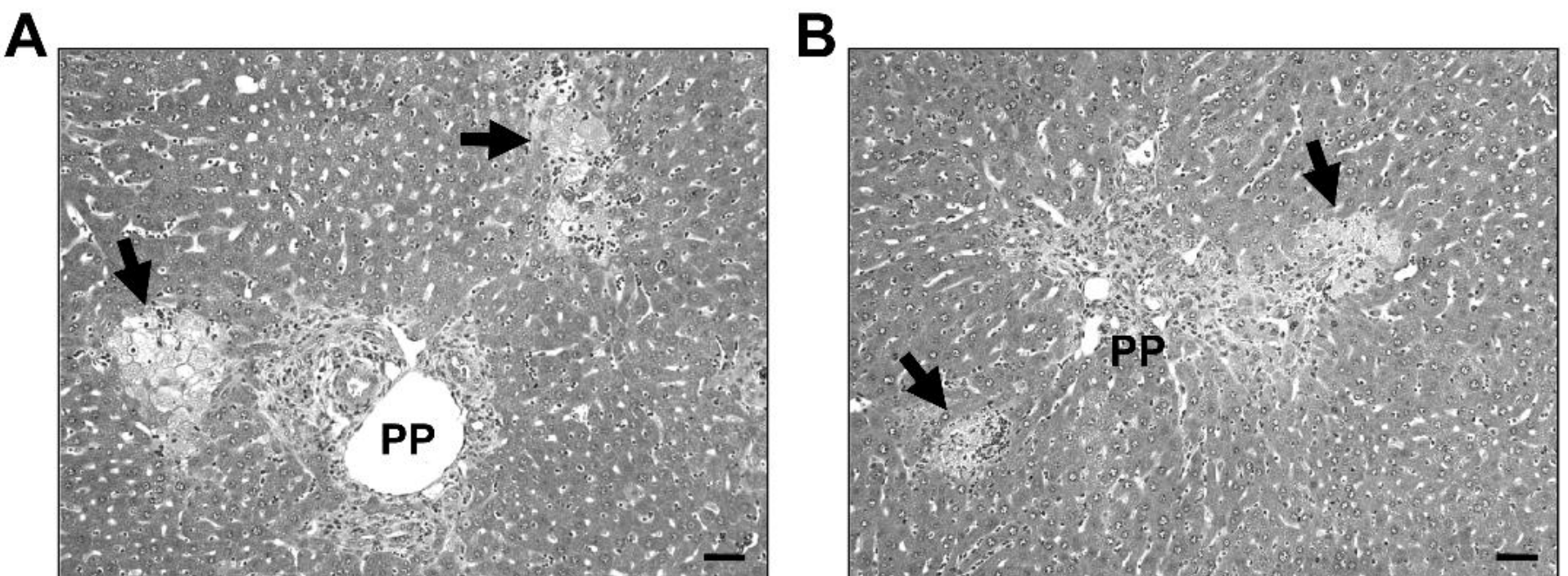

Figure 3

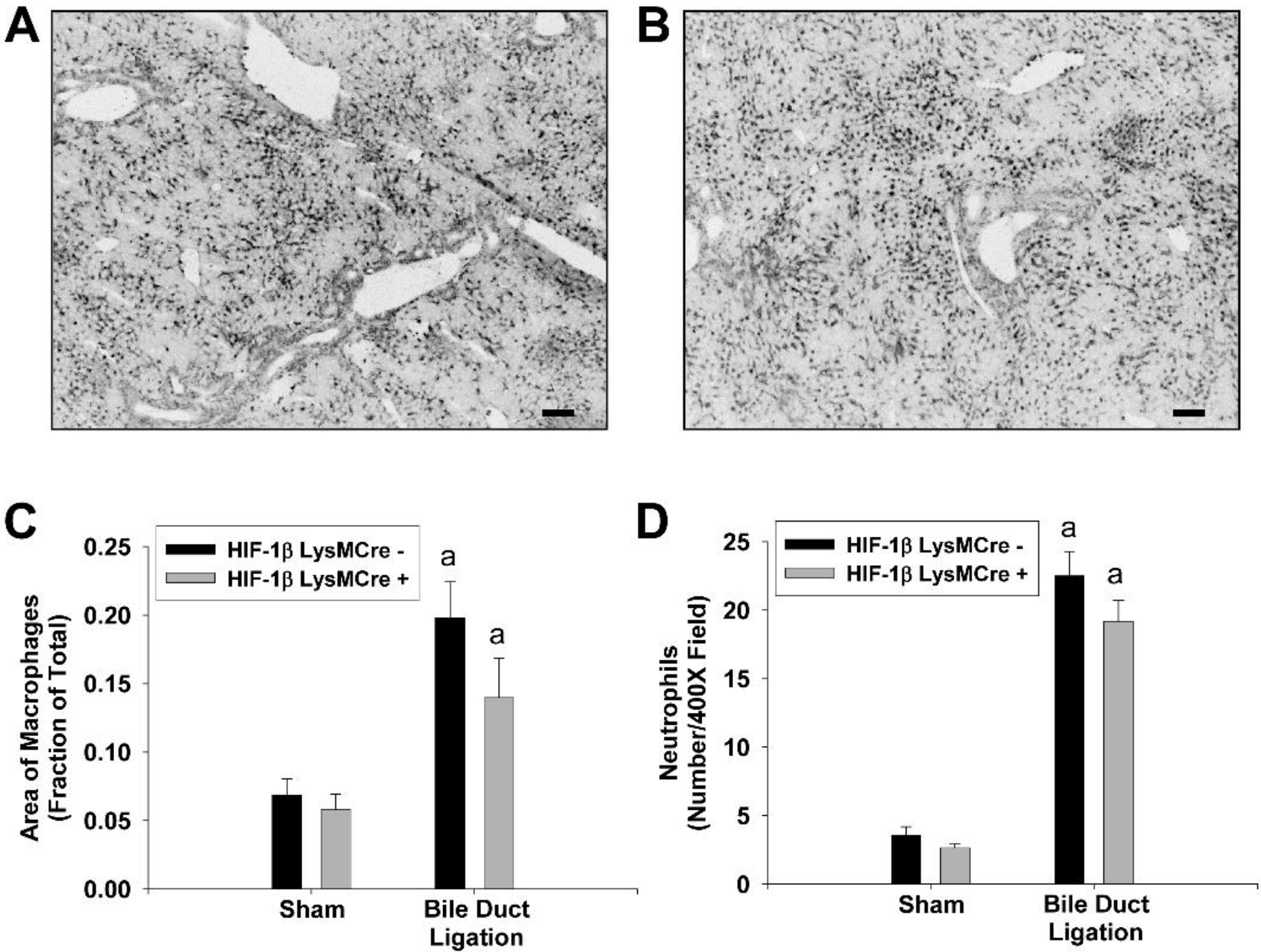
A
B
C
Area of Macrophages (Fraction of Total)
0.25
0.20
0.15
0.10
0.05
0.00
HIF-1β LysMCre -
HIF-1β LysMCre +
a
a
Sham
Bile Duct Ligation
D
Neutrophils (Number/400X Field)
25
20
15
10
5
0
HIF-1β LysMCre -
HIF-1β LysMCre +
a
a
Sham
Bile Duct Ligation

Figure 4

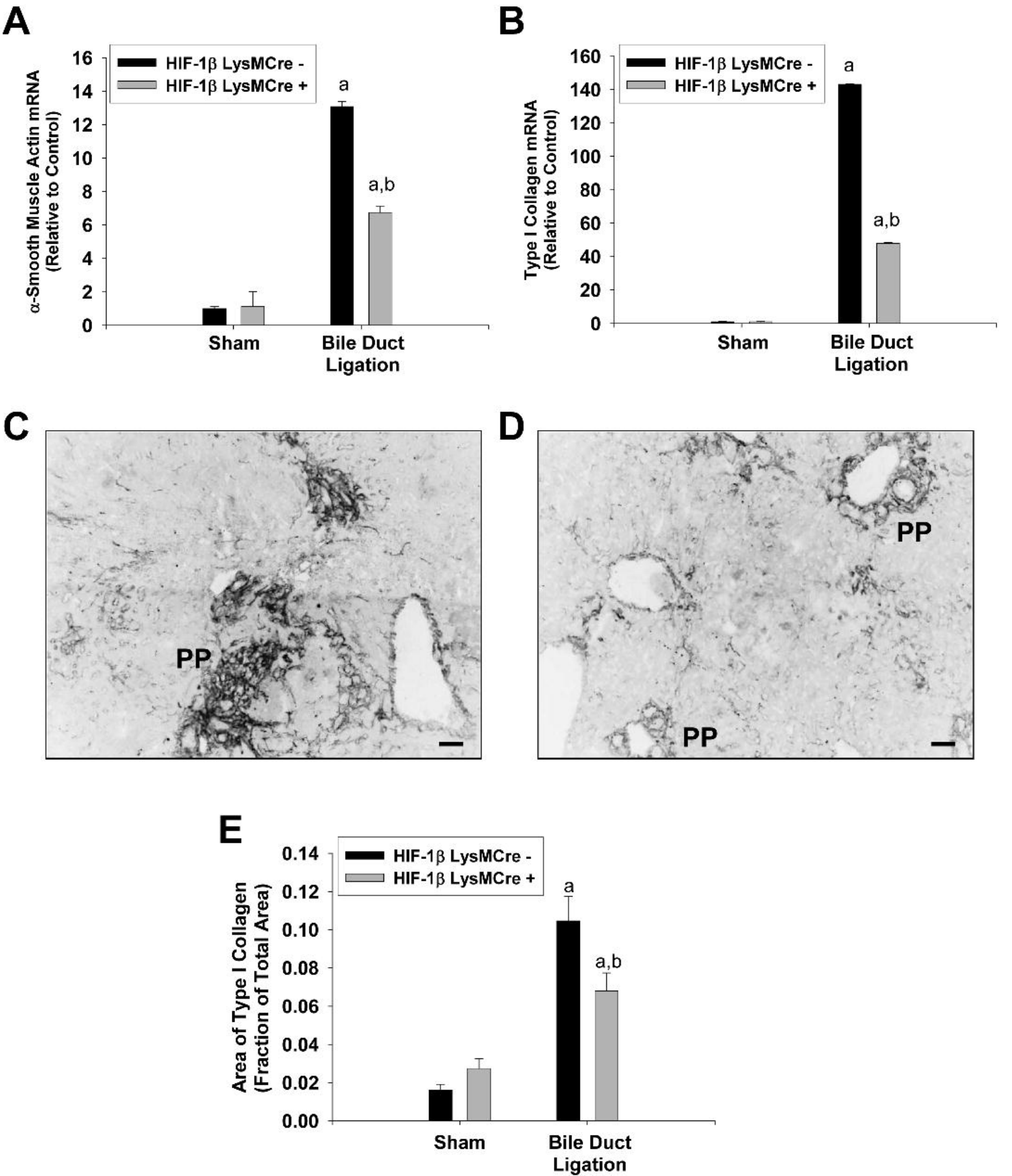
A
α-Smooth Muscle Actin mRNA (Relative to Control)
HIF-1β LysMCre -
HIF-1β LysMCre +
a
a,b
Sham
Bile Duct Ligation
B
Type I Collagen mRNA (Relative to Control)
HIF-1β LysMCre -
HIF-1β LysMCre +
a
a,b
Sham
Bile Duct Ligation
C
PP
D
PP
PP
E
Area of Type I Collagen (Fraction of Total Area)
HIF-1β LysMCre -
HIF-1β LysMCre +
a
a,b
Sham
Bile Duct Ligation

Figure 5

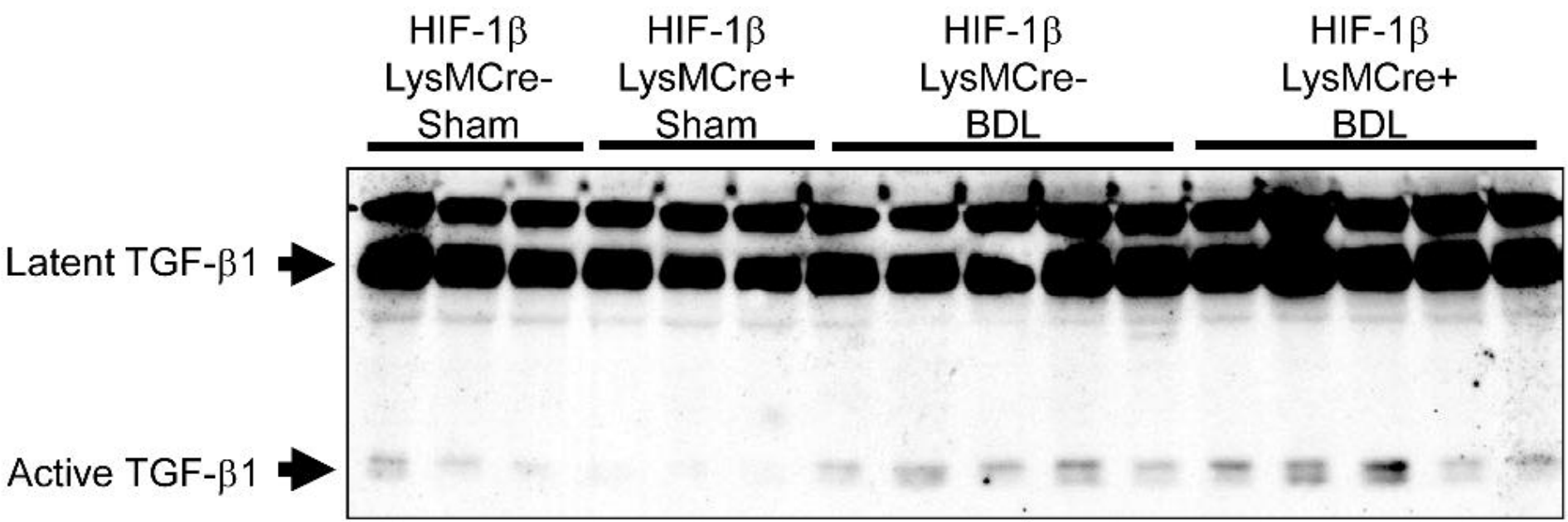
HIF-1β LysMCre- Sham
HIF-1β LysMCre+ Sham
HIF-1β LysMCre- BDL
HIF-1β LysMCre+ BDL
Latent TGF-β1
Active TGF-β1

Figure 6

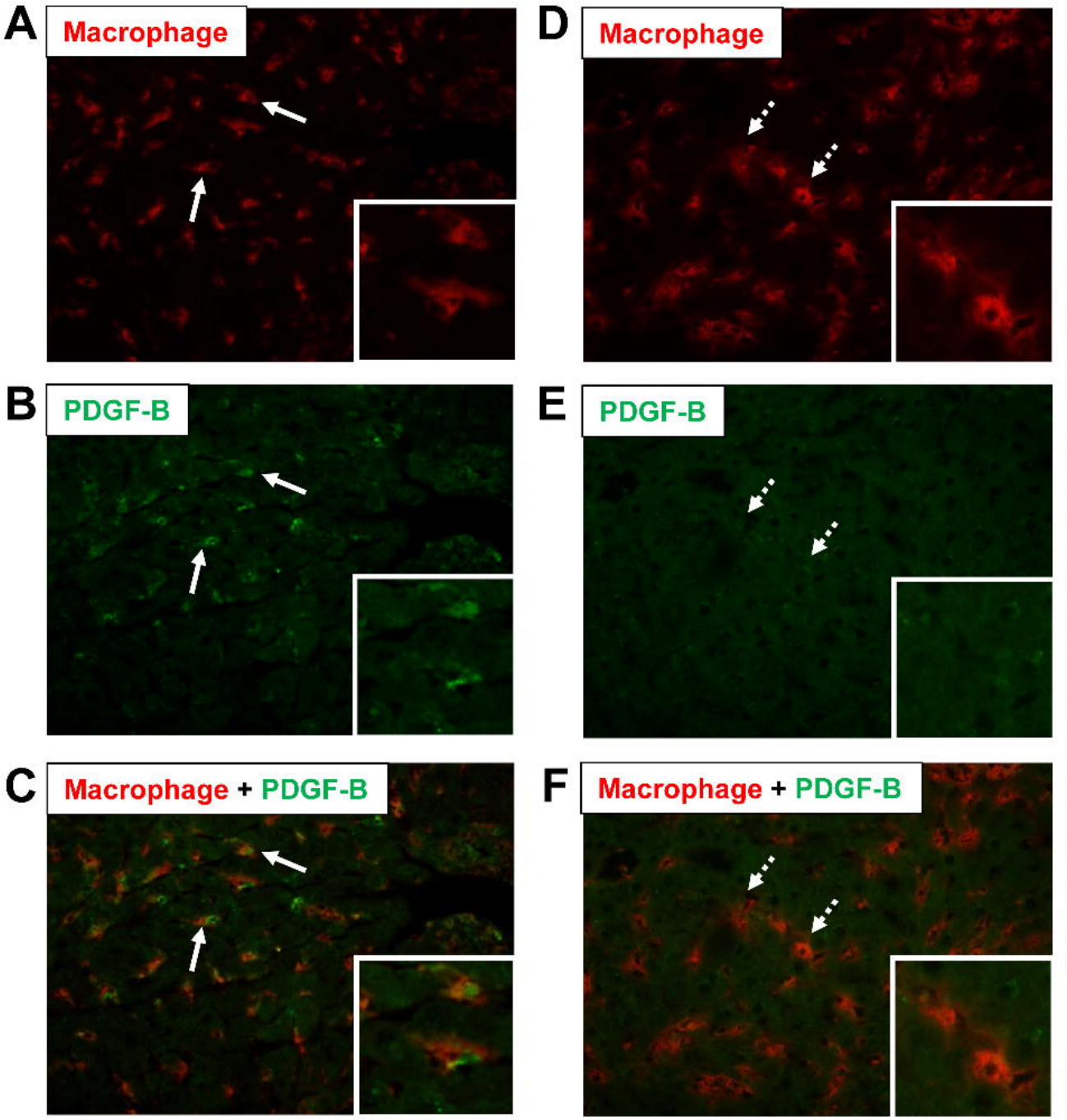
A
Macrophage
D
Macrophage
B
PDGF-B
E
PDGF-B
C
Macrophage + PDGF-B
F
Macrophage + PDGF-B

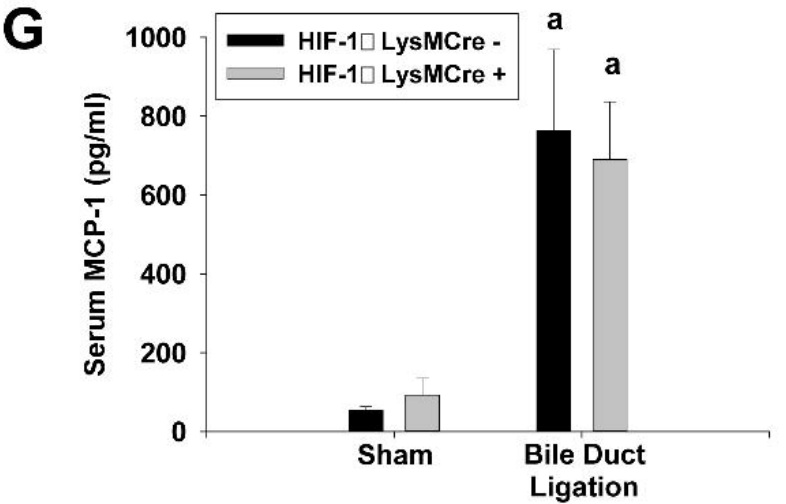
G
HIF-1□ LysMCre -
HIF-1□ LysMCre +
Serum MCP-1 (pg/ml)
1000
800
600
400
200
0
a
a
Sham
Bile Duct Ligation

Figure 7

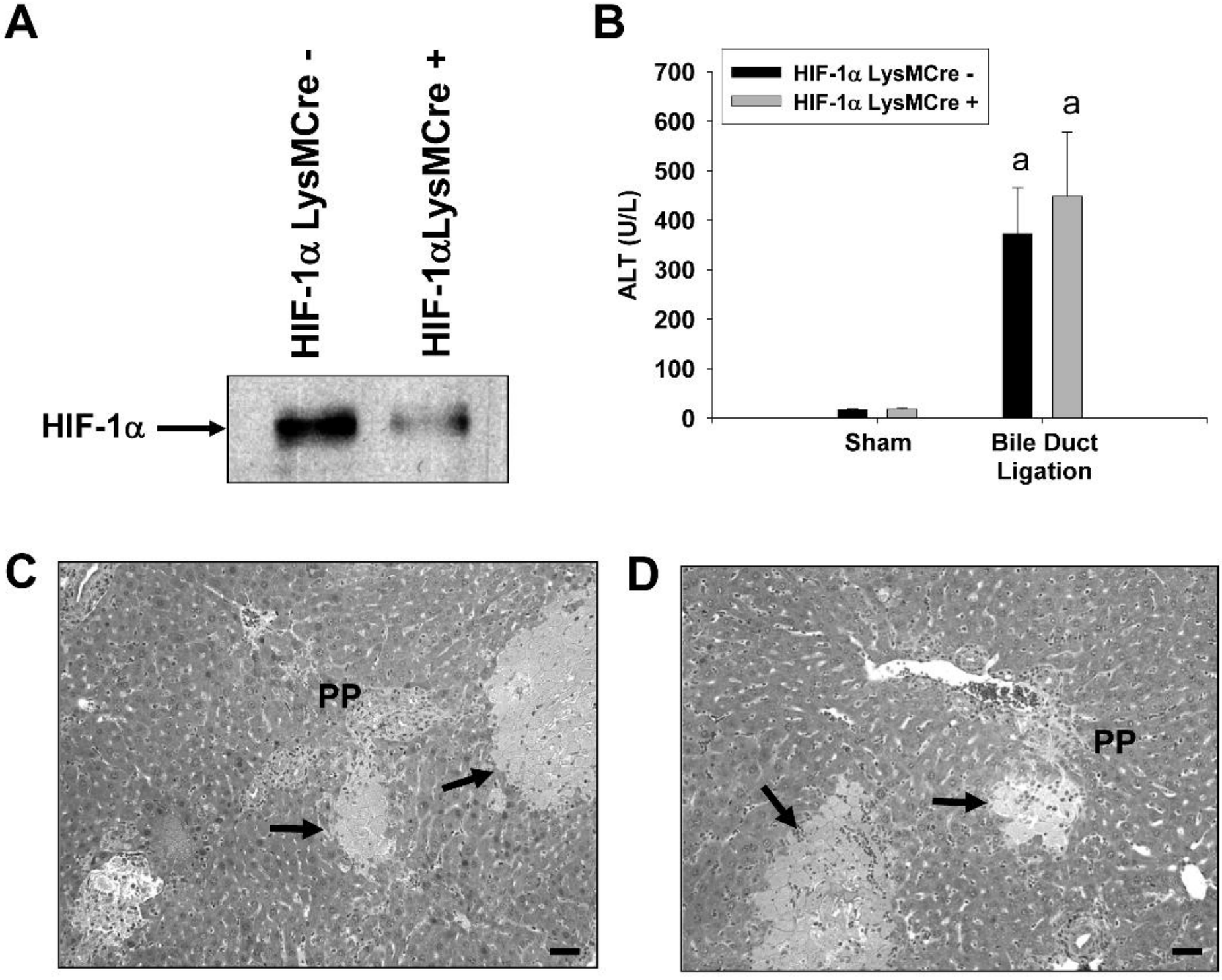
A
HIF-1α LysMCre -
HIF-1αLysMCre +
HIF-1α
B
HIF-1α LysMCre -
HIF-1α LysMCre +
ALT (U/L)
700
600
500
400
300
200
100
0
a
a
Sham
Bile Duct Ligation
C
PP
D
PP

Figure 8

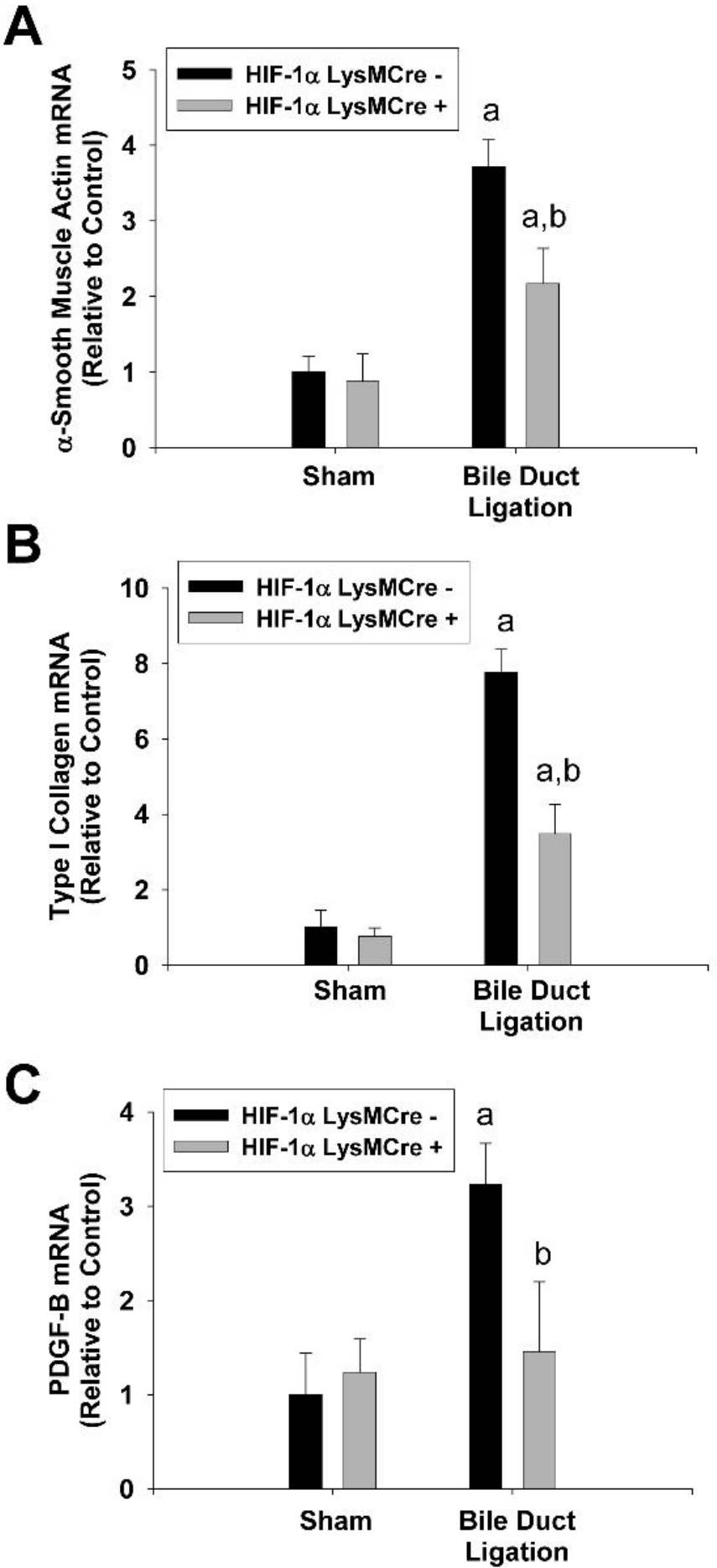
A
α-Smooth Muscle Actin mRNA (Relative to Control)
HIF-1α LysMCre -
HIF-1α LysMCre +
a
a,b
Sham
Bile Duct Ligation
B
Type I Collagen mRNA (Relative to Control)
HIF-1α LysMCre -
HIF-1α LysMCre +
a
a,b
Sham
Bile Duct Ligation
C
PDGF-B mRNA (Relative to Control)
HIF-1α LysMCre -
HIF-1α LysMCre +
a
b
Sham
Bile Duct Ligation

Figure 9

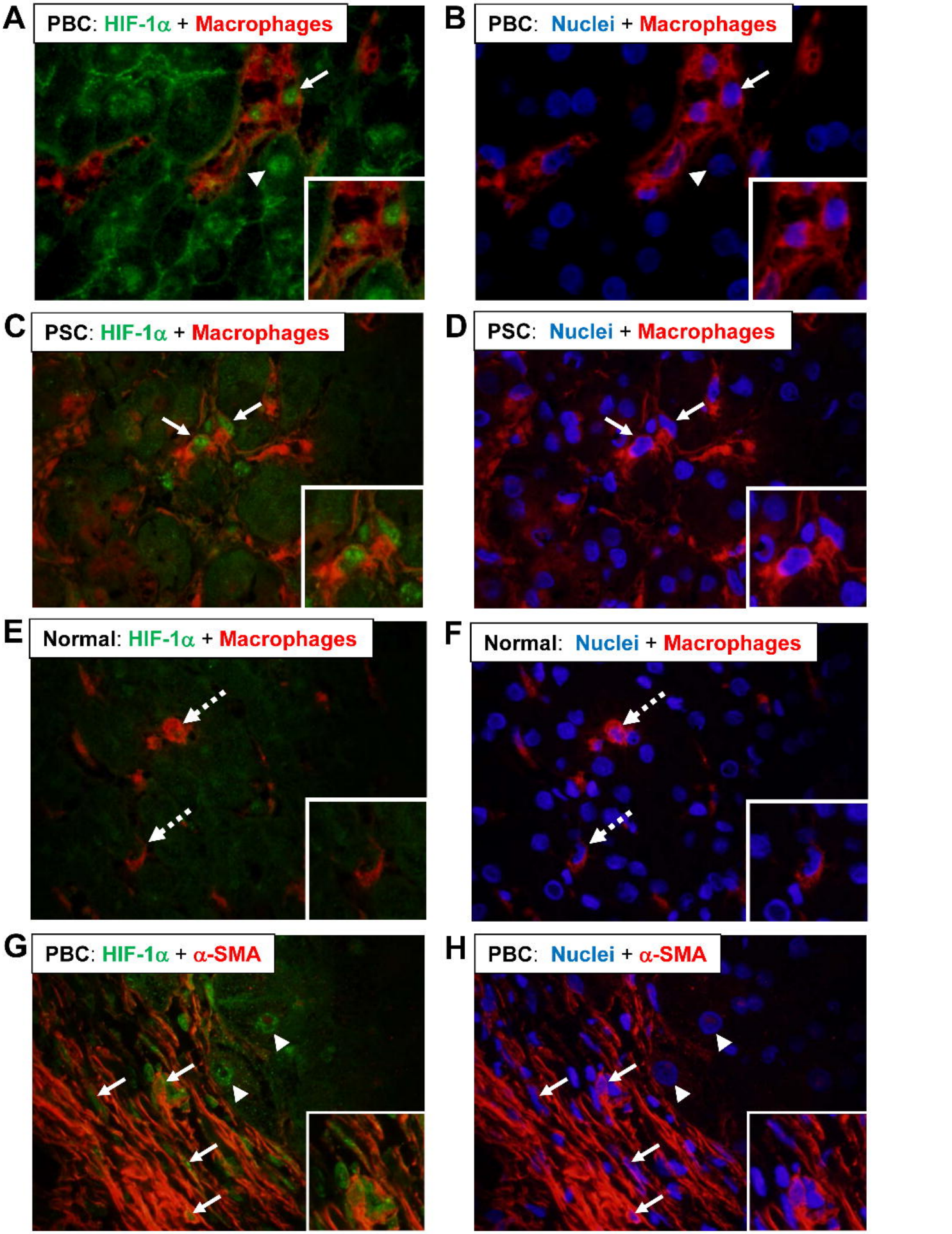
A
PBC: HIF-1α + Macrophages
B
PBC: Nuclei + Macrophages
C
PSC: HIF-1α + Macrophages
D
PSC: Nuclei + Macrophages
E
Normal: HIF-1α + Macrophages
F
Normal: Nuclei + Macrophages
G
PBC: HIF-1α + α-SMA
H
PBC: Nuclei + α-SMA